Light Metals 2015
Edited by: Margaret Hyland
TMS (The Minerals, Metals & Materials Society), 2015

A MODEL BASED STUDY OF CELL ELECTRICAL PREHEATING PRACTICES AT DUBAL

Alexander Arkhipov[1], Abdalla Zarouni[1], Sergey Akhmetov[1], Lalit Mishra[1], Amal Al Jasmi[1]

[1]Emirates Global Aluminium, Jebel Ali Operations, PO Box 3627, Dubai, UAE

Keywords: Cell electrical preheat, Aluminum electrolysis cells, DX+ technology, ANSYS, mathematical modelling

Abstract

DUBAL has extensive experience with electrical preheat of cells and continuously works on preheat optimization. Previously, preheat improvements were made by trial and error on real cells. Recently DUBAL developed a mathematical model of cell preheat which helps to optimize preheat parameters. This paper focuses on development of the DUBAL cell preheat model in ANSYS and model validation on DX+ cells. Detailed measurements of temperatures and voltage drops were carried out throughout the cell preheat. The model is three dimensional and transient. It represents a quarter of the cell and predicts the evolution of temperature distribution, heat loss and voltage drops in different parts of the cell, including graphite preheat bed. Different configurations of graphite preheat bed were modelled and verified in practice during EMAL Potline 3 start-up.

Introduction

It is well known that cell preheat is an important stage in cell life. A good preheat will have a positive impact on early operation of the cell and cell life expectancy [1]. Consequences of a bad preheat were briefly described in an earlier paper [2].

DUBAL has extensive experience with electrical preheat of cells and continuously works on preheat optimization [2]. Electrical preheat has undergone significant changes over the years. Previously, preheat improvements were made by trial and error on real cells. That way of development is very slow and expensive. Mathematical modelling has helped a lot in understanding and development of preheat practices in recent years [3 - 4].

DUBAL has developed a mathematical model of cell electrical preheat. This paper describes the model application and validation on DX+ cell technology during the start-up of EMAL Potline 3 using different preheat graphite bed configurations.

Measurements

The comprehensive measurement plan which was developed for preheat of DX cells [2] was adapted to DX+ cells with some improvements. Detailed temperature and voltage drop measurements were carried out to assess preheat quality and to determine the resistance and resistivity of the graphite bed as well as contact resistances between the cast iron and anode and cathode blocks. The measurements were described in detail in [2]. Here, the list of measurements is given and additional measurements are described:

1) Cathode block surface temperatures in 7 positions across the cell on 5 transverse slices between anodes (Figures 1 and 2). These were measured automatically by thermocouples embedded 2.5 cm below the cathode surface and recorded with a data logger.

Figure 1. Pot preparation for measurements during preheat

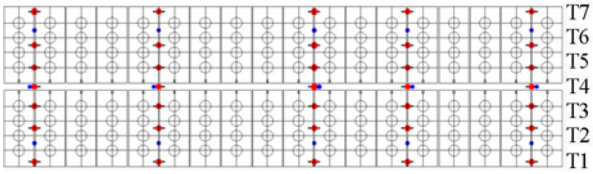

Figure 2. Locations for temperature and voltage measurements (blue points show voltage probe location, red ones show thermocouples)

2) Under hood gas temperature with 1 thermocouple fixed in the duct and connected to the data logger.
3) Cathode voltage drop and collector bar temperature on the same 5 cathode blocks, upstream and downstream (blue points in Figure 2 and red points in Figure 3). Three voltage probes were embedded below the cathode surface during anode installation. The voltage probe on the collector bars outside the potshell was a portable rod with pin.
4) Anode voltage drop from the rod below the clamp (by handheld voltage probe) to carbon side surface 5 cm above anode bottom (by fixed voltage probe) and outer stub temperature on 10 anodes close to temperature measurement sections [2].
5) Graphite bed voltage drops between the voltage probe on the side surface of the anode and two cathode surface voltage probes: central and upstream (US) or downstream (DS) depending on which anode was measured (Figure 3). This consists of graphite and parts of anode and cathode voltage drops.
6) External voltage drop, consisting of two parts: a) From each of the same 10 collector bars to the base of riser #1 of the next pot and b) From the base of riser #1 of the start-up pot to the rods below anode clamps of the same 10 anodes.
7) Potshell temperature approximately 25 cm above the collector bar at 10 locations, only once before bath-up.
8) Anode current distribution from voltage drops, measured with individual anode rod forks and recorded by data logger.

9) Cell resistance and amperage were obtained from Pot Control System one-minute data.

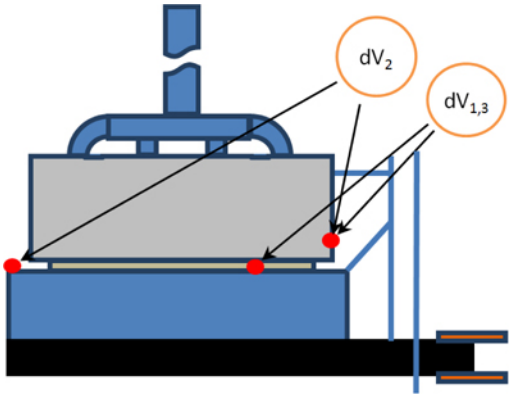

Figure 3. Graphite bed voltage drop measurements.

Another very important measurement which has to be done before preheat is a graphite bed compression test. The top and bottom width, length and height for each island were measured, but only top dimensions ("A" on Figure 4) are important in calculations because they define the zone under pressure which is the key factor for electrical resistivity of the graphite. The effective area and thickness of the graphite bed were determined by placing the anodes on the bed and measuring the compressed dimensions after anode removal (Table I).

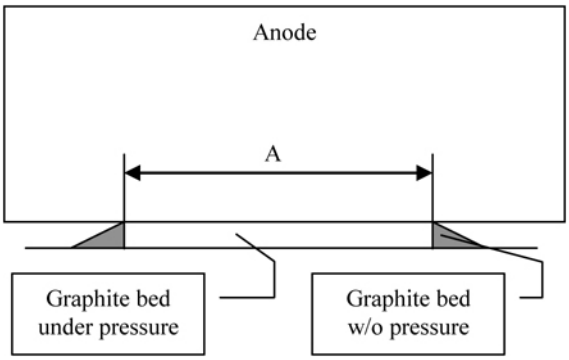

Figure 4. Shape of graphite bed under anode.

Table I. Data for compressed graphite islands.

	Island dimensions, mm		% anode coverage	
	Nominal	Compressed	Nominal	Compressed
Test 1	170x170x30	167x167x26	17.6	16.9
Test 2	142x142x30	154x154x20	12.3	14.5
Test 3	132x132x24	177x178x20	12.5	22.6
Test 4	600x140x24	615x155x20	13.1	14.9

Model development and validation

The basic DX+ cell preheat model was a slice, comprising one anode and 1.5 cathode blocks in order to decrease computer time (Figure 5a). This simplification was based on previous modelling results which showed insignificant impact of the end heat losses on the temperature field in the centre of the cell [3-4]. Final calculations were done using quarter model (Figure 5b).

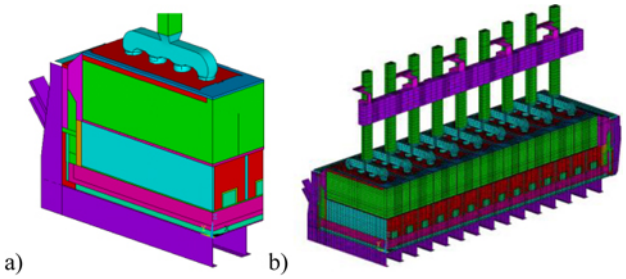

Figure 5. ANSYS preheat models: a) slice; b) quarter

The models consist of the cathode, prebaked anode with yoke and rod, part of anode ring busbar (only in quarter model) and graphite bed. The side channels and anode top are covered with crushed bath or anode cover recycled material (ACRM). Free space between the anodes and cathode surface is filled with air and on top covered by mineral wool. In order to simulate thermal and electrical contact resistance between cast iron of collector bars and cathode blocks and between cast iron of anode stubs and carbon, a bonded thermal and electrical contact behavior was set up in ANSYS using surface to surface contact elements ("bonded" contact surfaces cannot separate once contact is established).

Detailed description of boundary and initial conditions with corresponding equations was presented in [3]; here is the summary for both slice and quarter models:

1. Electrical current proportional to the size of the model is applied to the entrances on anode busbar in quarter model or to anode rod in slice model and zero electrical potential applied to cathode flexes.
2. Combined convection and radiation heat transfer coefficients are applied to all external surfaces.
3. Ambient temperature 30 °C was applied to all external surfaces outside the hoods. Inside the hoods, the ambient temperature increases from 30 °C at the beginning to 150 °C at the end of preheat.
4. Initial temperatures are equal to ambient temperature except for cathode block assembly in which they are 20-30 °C higher because some current flows through collector bars and cathode blocks as soon as they are connected to the busbars.

Physical properties for all materials (electrical resistivity, thermal conductivity, specific heat and density) were applied as a function of temperature. Transient runs for 56-60 hours of preheat time had the time step equal to one hour. Time step of 10 minutes was also checked but results did not show significant difference.

The most difficult part of the modelling was fine tuning of the contact resistances in the cathode and anode assemblies and of the electrical resistivity of the graphite bed. First run was made with zero contact resistance on cathode collector bars to carbon and anode stubs to carbon (Figures 6 and 7). Then calculated voltage drops were compared with measured ones and contact resistances as function of calculated temperature were applied. The temperature checkpoints were the measured temperatures on anode yokes and on the collector bars outside the shell.

After 2 iterations it appeared that proper contact resistance was found, for both anode stubs and collector bars. Model results show good agreement with measurements as can be seen in Figures 6 and 7.

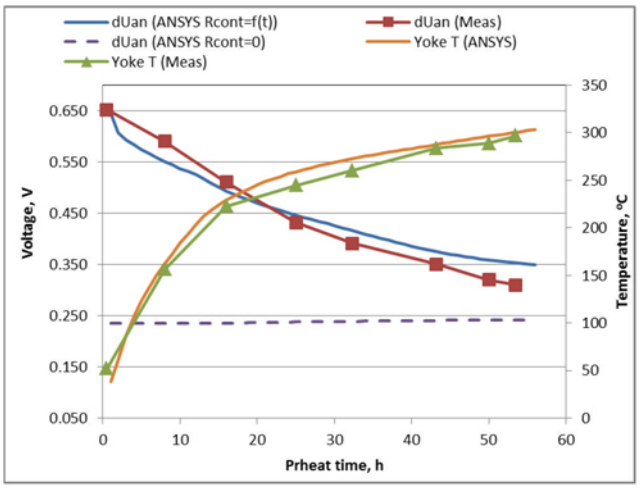

Figure 6. Calculated and average measured anode voltage drop and yoke temperature before and after contact resistance tuning.

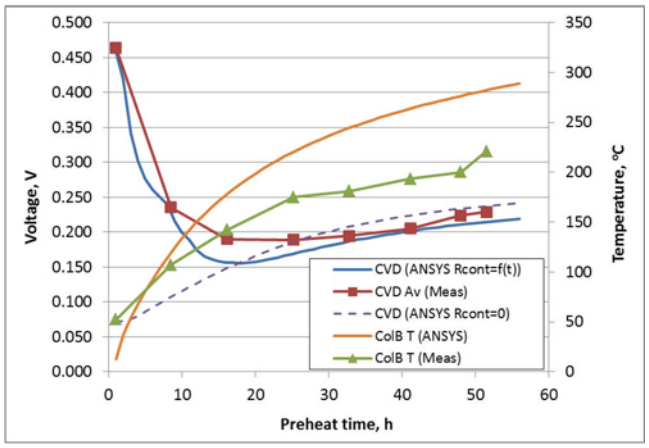

Figure 7. Calculated and average measured cathode voltage drop and collector bar temperature before and after contact resistance tuning.

Analysis of first modelling results has shown that graphite resistivity published previously [2] was significantly overestimated. The reason is very high electrical potential gradient along anode bottom surface and cathode top surface. For example, voltage drop between location at 5 cm above anode block bottom on its side (Figure 3) and center of interface area between anode bottom and top of graphite island can be a few hundred millivolts due to high concentration of current in the anode on top of graphite bed (Figure 8).

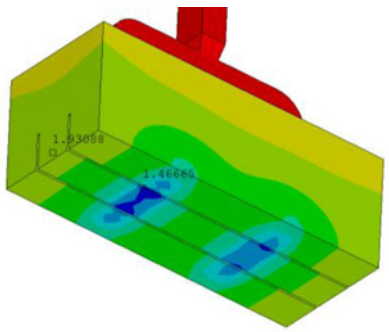

Figure 8. Modelled anode voltage drop during preheat

Also it is worth mentioning that electrical resistivity as specified in graphite or coke material certificates cannot be used for any calculation of the cell resistance during preheat or modelling. This is because suppliers usually measure the properties at very high pressure of about 3 MPa (for example R&D Carbon RDC 147 equipment, ISO 10143) and at room temperature only. But graphite or coke undergoes about 0.01-0.2 MPa pressure during preheat depending on percentage of anode coverage. The resulting suppliers' electrical resistivity is therefore much lower and cannot be used for any calculation. Another factor is contact resistance between graphite grains and carbon of anode and cathode blocks. For example, for coke it is shown in [4] that contact resistance between coke and cathode block equals 20 – 25 % of the resistance of 40 mm thick layer of coke.
Taking into account all this, initial graphite resistivity was set to a constant value of 687 μΩm. Comparison of results of first run with constant graphite bed resistivity is shown in Figure 9. It can be seen even this constant value of graphite electrical resistivity gives pretty good results on average.

Adjustment of graphite resistivity was done at different temperatures using following method:

1) Pure graphite voltage drops (pure means without anode and cathode parts) was calculated from ANSYS results at every point of time for which we had measured voltage drops.
2) Using the same modelling results, extra contributions to graphite bed voltage drop from anode and cathode parts was subtracted from every measured graphite bed drop to give measured pure graphite drop.
3) Initial graphite grains resistivity was multiplied by ratio between measured and modelled pure graphite voltage drop at every measurement time.
4) Electrical resistivity of graphite grains was set in ANSYS as function of temperature in a table. For each value of resistivity the average temperature of cathode surface at that moment was applied. But modelling results show that graphite bed voltage drop curve lags the measured one. This is because measurements on the cathode surface were done between anodes where the temperature is lower than inside the graphite bed layer under anodes. To fix this issue, the temperature in the resistivity of graphite grains was increased by a factor of 1.2. After this adjustment, the calculations came much closer to measurements (Figure 9). Final resistivity which was used in calculation is shown in Figure 10.

Increase of graphite resistivity above 800 °C is most probably caused by graphite bed burn and not material property changes.

Comparison of measured and modelled surface temperatures in different locations is shown in Figure 11. Temperatures were measured in 7 locations on 5 sections. For comparison section 1 and 5 were not taken into account because only central section was modelled. US and DS (1 - 7, 2 - 6, 3 - 5 on Figure 2) points were considered as same points due to symmetry.

Slice modelling results

After the model had been validated, several graphite templates were studied. The templates differ by number, shape and orientation of graphite islands under anodes and also by area coverage. Templates 1 - 5 have different arrangement of graphite under anodes with 13% of anode coverage. Templates 6 and 7 have 1

large graphite island which covers 40 % and 30 % of anode respectively. The resistivity of graphite for templates 6 and 7 increased by a factor of 2.

Results for all cases were thoroughly analyzed. Using special ANSYS macros the following parameters were calculated and combined in Table II: average cathode surface temperature, average volume temperature of cathode blocks and inter blocks seams, maximum and minimum cathode surface temperature, maximum temperature gradient in cathode blocks and average temperature gradient on cathode blocks surface, average and standard deviation of surface temperature.

Temperature fields for a few cases are shown Figure 12. From modelling results it can be concluded that templates which have more islands under each anode give more uniform temperature distribution and much less local overheat. But a further increase of the number of islands does not have a significant impact on results (Templates 4 and 5. Table II).

Some graphite bed shapes and orientations give more uniform temperature distribution than others, as can be seen from standard deviation of surface temperatures, but generate less heat with the same area of bed due to more uniform current distribution in the anode (Template 2 in Table II).

Templates with one large resistor island show as good results as the case with many islands in terms of temperature uniformity but the problems are: 1) To find twice more resistive material, 2) Amount of graphite to be skimmed after bath-up and 3) If contact resistance gives similar contribution as in case of coke usage than twice higher resistivity will not be sufficient.

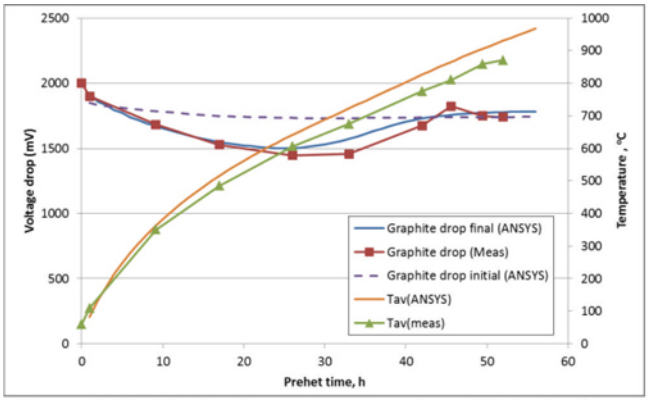

Figure 9. Modelled and average measured graphite bed voltage drop and average cathode surface temperature before and after graphite resistivity adjustment.

Different templates with almost the same percentage of anode coverage require different height of graphite bed due to different anode and cathode voltage drop (mostly anode drop).

Despite of the fact that for different templates different thickness of graphite bed was used, the compression tests show that the thickness of graphite is not a very practical parameter to adjust especially for islands with small area. Also it appears that high contribution of contact resistance to overall resistance of graphite bed makes the increase of overall resistance due to bed thickness increase much smaller than expected. Therefore, it is better to increase the resistance of the bed by adjustment of the area.

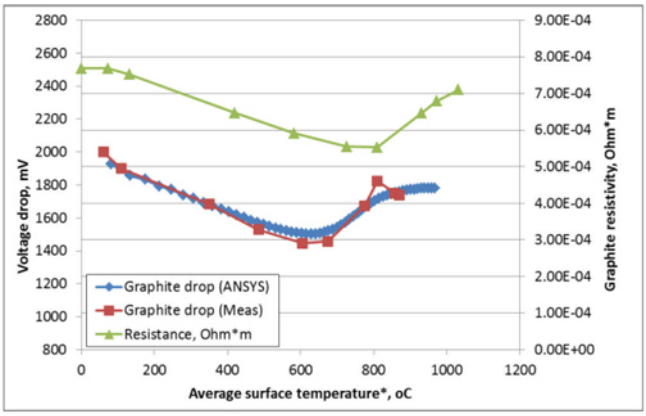

Figure 10. Calculated resistivity of graphite grains and comparison of measured and modelled graphite bed voltage drop.

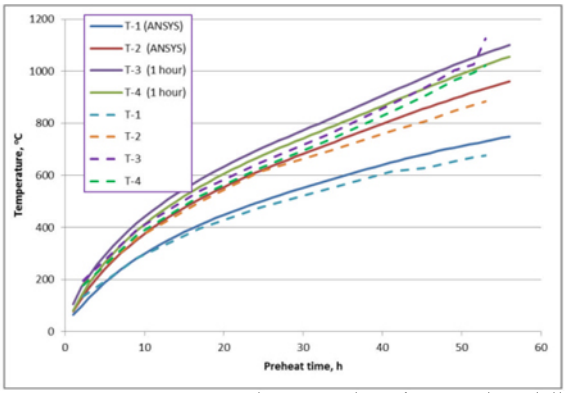

Figure 11. Average measured (3 central sections) and modelled

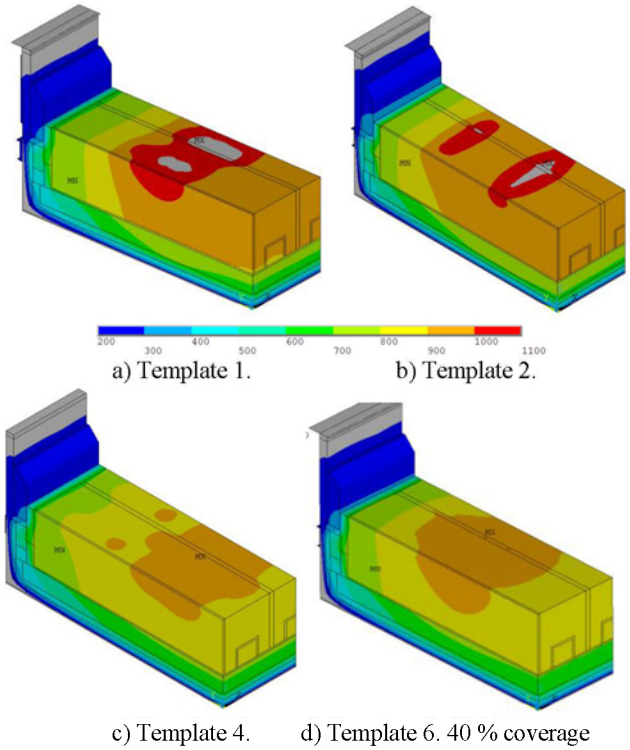

a) Template 1. b) Template 2.

c) Template 4. d) Template 6. 40 % coverage

Figure 12. Temperature fields for four templates.

As it was mentioned above, final calculations were done on quarter model (Figure 2b) to see overall temperature distribution across cathode. In quarter model, anode ring and preheat flexes were added to have correct current distribution across anodes. As reported in previous work [3, 4], end cathode blocks can have much lower temperature and current flow through corner anodes can change with time. Flexes have to be included in the model because they add significant resistance to overall current flow and flatten current distribution between anodes. Additional voltage drop due to preheat flexes was measured during preheat and found to be about 170 mV for DX+ cells in EMAL Potline 3. Flexes were modelled so that they gave measured voltage drop.

Quarter model results for Template 2 show that at the end of preheat the last 2 cathode blocks have much lower temperature (Table III) and the same was observed from measurements. This difference, which is above 100 °C, can lead to overheating of the cell during preheat because for usual preheat practice, process control staff uses measurements of cathode surface temperature only at the second and the last but one block to judge preheat quality.

To solve this issue, the graphite islands cross section under 1st and 2nd anode near the ends was increased 1.5 times to allow more current through two corner anodes in each quarter. This gave almost the same surface temperature in the centre of block #2 (Figure 14). Temperature increase of 1st block up to same value as central blocks is not possible without significant overheating of blocks #2 and #3.

Table III. Comparison quarter model results

Case #	Template 2		
	All equal	Corn. 1.5x	Corn 1.5x
Cover thickness, cm	**8**	**8**	**4**
Graphite thickness*, mm	**25**	**28***	**28**
Central anodes coverage, %	13.1%	11.9%	11.9%
Corner anodes coverage, %	13.1%	17.5%	17.5%
Average anode coverage, %	13.1%	13.1%	13.1%
Surface avg. temp, °C	**860**	**930**	**921**
Cathode avg. temp, °C	**843**	**909**	**909**
Center temp. of block #1	704	809	-
Center temp. of block #2	776	893	-
Center temp. of block #8	873	917	-
Center temp. of block #16	869	911	-
Total power at 56 h, kW	-	1075	1088
Anode heat loss, kW/ %	-	259 / 24	290 / 27
Cathode heat loss, kW/ %	-	267 / 25	263 / 24

Graphite bed under corner anodes should not be increased by 1.5 times compared to the base case with equal islands for all anodes because it will lead to increase of total graphite bed area and lower average preheating temperature. Calculations show that in case of 36 anodes, the cross-sections of all graphite islands under central anodes have to be decreased by 10 % and graphite bed under corner anodes has to be increased by 35 % in comparison with original graphite area or by 50 % comparing with new area of graphite under central anodes. Quarter model of Template 4 shows the same results. Template 4 with different central and corner graphite islands was recommended for DX+ cells preheat in EMAL Phase II and successfully implemented [5].

Another point of interest was impact of anode top insulation on preheat temperature. Anode cover thickness was decreased from 8 to 4 cm but there was almost no difference in final cathode temperature. In fact even at the end of preheat, heat loss from cell is about 50 % of heat generated and the rest is being absorbed by pot materials as they are heating up. For the same reason, the heat loss from the pot is zero at the beginning of preheat. According to Table III, we can roughly assume that 2 % more total heat loss at the end of preheating due to lower anode cover thickness would give 1 % more heat loss on the average during the whole preheat. This would decrease the final cathode temperature by 9 °C only.

Model validation

Many measurements were made during preheat in DX+ EMAL Phase II and DX DUBAL Potline 8 cells to validate the model. Measurements confirm the modelling results. As can be seen on Figure 15 Template 2 gives more even temperature distribution than Templates 1 and 3.

The same approach was used for DX+ Ultra preheat modelling to adjust Template 4 with increased corner island. Predicted average temperature for 35 surface thermocouples agreed well with average temperature measured in same locations (Figure 13).

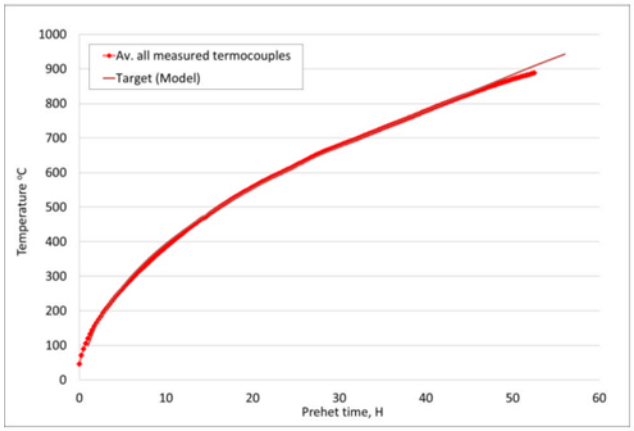

Figure 12. Predicted and measured average surface temperature during preheat DX+ Ultra cell 277.

Conclusions

Results of DX+ cell preheat model developed in DUBAL show very good agreement with measurements. The model helped improving existing preheat practices at EMAL and DUBAL.

Modelling and measurements show that:

1) Preheat template with higher number of graphite islands gives the best results and it was implemented in EMAL and DUBAL.
2) Most probably, thickness of graphite bed is not an effective factor to regulate heat generation in the preheating cell.
3) Anode cover thickness does not impact significantly the preheat temperature.
4) To have temperature of end blocks closer to the centre ones, the area of graphite bed under 8 corner anodes has to be 1.5 times greater than the area under central anodes.
5) Anode voltage drop can change significantly with the change of preheat template and this change has to be taken

into account in estimation of overall heat generation during preheat.

6) Compression test is a very important check when preheat template is changed, especially for templates with relatively small area of each island, because the initial graphite bed area can change considerably and the effect of template change can be opposite to expected one.

Acknowledgements

The authors thank all other people who participated in this development and particularly Dr. Ali Al Zarouni, Mahasal Khan, Abdulla Al Jaziri, Rawa Ba Raheem, Nadia Ahli, Aslam Khan, Vijaya Kumar as well as the very dedicated measurement teams of DUBAL and Emal Process Control and Technology Development & Transfer Department.

References

1. M. Sørlie, Harald A. Øye, *Cathodes in Aluminium Electrolysis*, 3rd Edition, Aluminium Verlag 2010, 111-181.
2. A. Arkhipov et al., "Cell electrical preheating practices at DUBAL", *Light Metals* 2014, 445-449.
3. A.G. Arkhipov and P.V. Polyakov, "Calculation of aluminium cells in preheating, start-up and post-start-up period", *Proc. Conference Aluminium of Siberia 2004*, 2004, 149-163.
4. A. Arkhipov and P. Polyakov, "A modelling based study of technological and design parameters impact on cathode lining integrity during electrical and flame preheat". *11th Australasian Aluminium Smelting Technology Conference*, 2014, to be published.
5. W. Alsayed et al., "World's longest potline start-up at EMAL", *Light Metals* 2015.

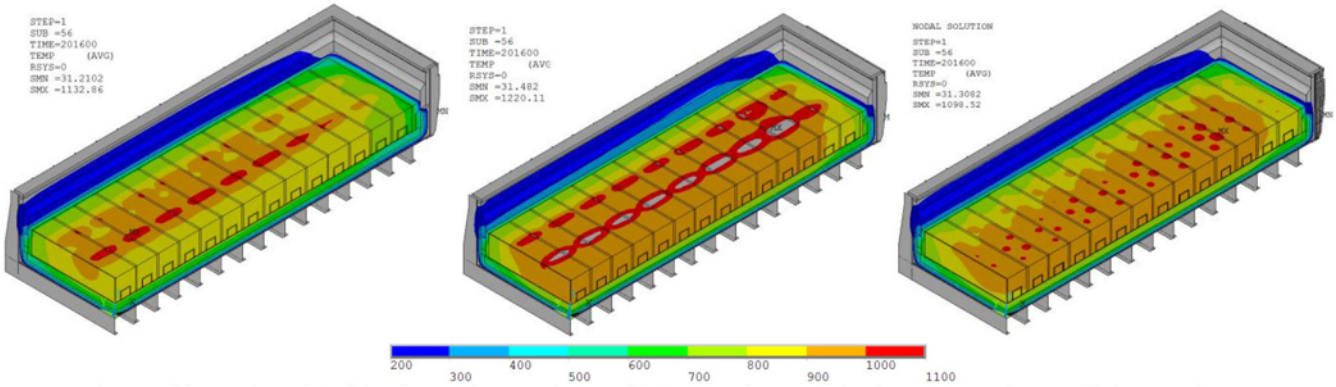

a) Template 2 with equal graphite islands b) Template 2 with increased corner islands c) Template 4 with increased corner ones

Figure 14. Modelled temperature fields for different templates

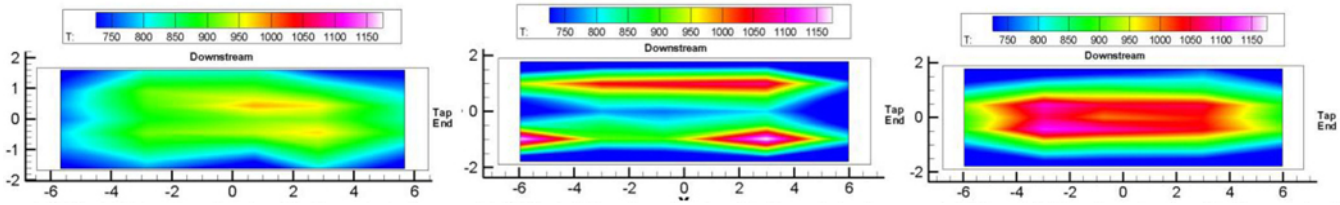

a) DX at 52 h of preheat with Template 2 b) DX at 43 h of preheat with Template 1 c) DX+ at 54 h of preheat with Template 3

Figure 15. Measured temperature fields for different templates.

Table II. Modelling result of cell preheat with different templates

	Template 1	Template 2	Template 3	Template 4	Template 5	Template 6	Template 7
Graphite thickness, mm	22	25	25/28	25	25	44	33
Average cathode surface T, °C	923	931	980	869	865	881	832
Average cathode volume T, °C	909	920	960	855	850	886	819
Min. top surf. T, °C	655	694	681	628	643	671	642
Max. top surf. T, °C	1156	1201	1272	977	967	1012	967
T in center channel, °C	912	919	1005	878	893	850	805
SD of cathode surface T, °C	131	94	136	75	74	75	67
Max. T grad. in block, °C/mm	1.40	1.86	2.1	0.96	1.045	0.812	0.67
Average T grad., °C/mm	0.45	0.47	0.50	0.32	0.32	0.33	0.30
Anode block voltage drop, mV	668	561	599	595	437	-	-
Energy, kWh	65938	65979	67775	61467	62339	64039	59703